AEDC-TR-68-211

PERFORMANCE OF A DYNAMICALLY COMPENSATED LOAD CELL FORCE MEASUREMENT SYSTEM

F. L. Crosswy and H. T. Kalb

ARO, Inc.

November 1968

ARNOLD ENGINEERING DEVELOPMENT CENTER
AIR FORCE SYSTEMS COMMAND
ARNOLD AIR FORCE STATION, TENNESSEE

NOTICES

When U. S. Government drawinga apecifications, or other data are uaed for any purpose other than a definitely related Government procurement operation, the Government thereby incura no responsibility nor any obligation whatsoever, and the fact that the Government may have formulated, furnished, or in any way aupplied the said drawings, apecifications, or other data, ia not to be regarded by implication or otherwiae, or in any manner licenaing the holder or any other person or corporation, or conveying any righta or permiaaion to manufacture, uae, or aell any patented invention that may in any way be related thereto.

Qualified uaera may obtain copiea of this report from the Defenae Documentation Center.

References to named commercial producta in thia report are not to be conaidered in any sense as an endoraement of the product by the United States Air Force or the Government.

PERFORMANCE OF A DYNAMICALLY COMPENSATED LOAD CELL FORCE MEASUREMENT SYSTEM

F. L. Crosswy and H. T. Kalb
ARO, Inc.

FOREWORD

The work presented herein was sponsored by Arnold Engineering Development Center (AEDC), Air Force Systems Command (AFSC), Arnold Air Force Station, Tennessee, under Program Element 62302F, Project 5730, Task 04.

The results of the work were obtained by ARO, Inc. (a subsidiary of Sverdrup & Parcel and Associates, Inc.), contract operator of AEDC, under Contract F40600-69-C-0001. The research and testing were performed from August to October, 1967, under ARO Project No. BC5820, and the manuscript was submitted for publication on August 28, 1968.

This technical report has been reviewed and is approved.

Forrest B. Smith, Jr.
Research Division
Directorate of Plans
and Technology

Edward R. Feicht
Colonel, USAF
Director of Plans
and Technology

ABSTRACT

This report presents a theoretical description and an experimental evaluation of a dynamically compensated load cell force measurement system. Electronic compensation techniques were used to eliminate load cell signal distortions caused by large amplitude load cell base (thrust butt) motions and other structural transient responses of the force measurement device. The force measurement device was subjected to severe impact forces up to 4600 lb peak force with force rise times of 300 μsec and total force durations of 900 μsec. Load cell base motions caused by these impact forces approached 0.25 in., and the load cell signal was badly distorted. However, application of the compensation techniques eliminated these distortions, and dynamic force measurements could then be made regardless of load cell base motion and the structural response of the rest of the force measurement device.

CONTENTS

APPENDIX

Illustrations

SECTION I
INTRODUCTION

Static forces can be accurately and precisely measured with a conventional load cell device. However, dynamic forces can excite the natural frequencies of the mechanical structure attached to the load cell and thereby distort the load cell signal. Therefore, the essence of the dynamic force measurement problem is to develop techniques to eliminate these transient distortions from the load cell signal. An electronic compensation technique has been developed than can eliminate distortions caused by several degrees of freedom of the force measurement system (Refs. 1 through 3).

The compensation technique utilizes the summation of the load cell signal and an accelerometer signal to eliminate the distortion caused by the first mode natural frequency. This summation procedure is referred to as the "reaction force summation technique." Next, the inverse transfer function of the measurement system structure is formed with operational amplifier circuitry and is used to operate on the output signal of the reaction force summation circuitry to eliminate the load cell signal distortions caused by the second and higher mode natural frequencies. This transfer function compensation procedure is sometimes called the "computer compensation technique" since the circuitry used is actually that of a special purpose analog computer. This "hybrid" combination of the reaction force summation technique and the computer compensation technique has been shown to be quite effective for eliminating load cell signal distortions caused by the transient structural response of an experimental thrust stand (Refs. 1 through 3). The hybrid compensation technique was specifically developed for use with rocket thrust stands, but the principles involved are applicable to many other dynamic measurement systems (Ref. 2).

The purpose of this report is to provide (1) theoretical bases for application of dynamic compensation techniques and (2) experimental data that illustrate the effectiveness of the hybrid compensation technique for elimination of load cell signal distortions caused by (a) load cell base motions and (b) transient response of the structure forward of the load cell base.

SECTION II
APPARATUS

2.1 IMPACT FORCE MEASUREMENT DEVICE

A schematic of the impact force measurement device is shown in Fig. 1, Appendix I. The basic force measurement transducer is a 5000-lb rated load cell. A steel accelerometer housing is rigidly attached to the active end of the load cell. The accelerometer mounted in the housing is an undamped piezoelectric type with a mounted resonant frequency of 27,000 Hz. Rubber-cork material is mounted on top of the housing to control the impact characteristics of the impacting sphere since a metal-to-metal impact could produce a peak force of several hundred thousand pounds. A steel sphere weighing 2.31 lb is dropped on the rubber-cork material to produce the impact force. The sphere is magnetically supported by an electromagnet solenoid device and is released when the current to the solenoid is interrupted. The height of the sphere is adjustable from 3 to 20 ft. A light source and collimator are used to position a thin beam of light 0.25 in. above the rubber-cork material. A photodiode and associated circuitry is positioned opposite the light source and is used to detect the presence of the light beam. When the sphere interrupts the light beam, the photodetector device produces a voltage pulse which, in turn, initiates the sweep on an oscilloscope. Oscilloscope photographs were used to record all data.

The base of the load cell is attached to a cantilever beam. The cantilever beam is welded to a massive, braced, I-beam structure which is, in turn, bolted to the concrete floor. A linear, variable, differential, transformer (LVDT) with microinch resolution capability is used to monitor the motion of the cantilever beam and load cell base. The LVDT is calibrated with a micrometer dial with 0.0001-in. divisions. A steel block is used to brace the cantilever beam to alter its dynamic response as compared to the unbraced condition. The dynamic response characteristics of the cantilever beam differ significantly between the blocked and unblocked conditions. The primary object of the impact force-load cell base motion experiment is to show that the use of the hybrid compensation technique permits accurate dynamic force measurements to be made regardless of the dynamic response characteristics of the load cell base support structure. Experimental demonstration of this fact would then permit the use of hybrid compensation techniques to eliminate rocket thrust data distortions caused by thrust butt motions.

2.2 FORCE MEASUREMENT AND DYNAMIC COMPENSATION CIRCUITRY

A block diagram of the instrumentation and dynamic compensation circuitry, which comprises the hybrid static and dynamic force measurement system, is shown in Fig. 2. The basic force transducer is a conventional load cell with a maximum force rating of 5000 lb. Load cell electrical excitation is furnished by a conventional voltage-regulated power supply. The accelerometer is an undamped piezoelectric type with a mounted resonant frequency of 27,000 Hz. The accelerometer signal is fed to a conventional charge amplifier which, in turn, furnishes one input signal to the summing amplifier. The load cell signal furnishes the other signal to the summing amplifier. The output of the summing amplifier furnishes the input signal to the linear phase filter, which is a Bessel type with a variable cutoff frequency (100 to 10,000 Hz) and an attenuation rate of 18 db per octave. The computer compensator is an approximate differentiator type (Ref. 1) with a natural frequency compensating range from 20 to 2000 Hz and a damping ratio compensating range from 0 to 1.0. The gain amplifiers and the summing amplifier are formed from differential operational amplifiers with a unity gain-bandwidth product of 2 MHz. The digital voltmeter has an ultimate resolution of 1 mv and is used in the force measurement calibration procedure. The null indicating voltage standard has an ultimate resolution of 20 μv and is also used in the calibration procedure.

SECTION III
THEORETICAL CONSIDERATIONS

The theoretical bases for application of dynamic compensation techniques are presented in this section.

3.1 FORMULATION OF THE MECHANICAL MODEL

It should be stated at this point that the purpose for formulating a model of the force measurement system structure is not to ultimately calculate the transient and steady-state response variables but to provide an intuitive and theoretical basis for the application of dynamic compensation techniques. It is, therefore, not important to formulate a precisely accurate model of the structure.

All mechanical structures are fabricated with continuous mass components and in some cases can be successfully analyzed only by

distributed parameter techniques. However, a time-invariant, lumped parameter model is entirely adequate for the purposes of this analysis. The static and dynamic responses are, therefore, describable by ordinary, linear, differential equations with constant coefficients.

When dynamically excited, the force measurement structure, schematically shown in Fig. 1, exhibited three appreciable amplitude natural frequencies. For the purposes of this study an appreciable amplitude natural frequency is defined as one with an amplitude large enough to require compensation. With the load cell base and cantilever beam in the blocked condition, the observed natural frequencies occurred at about 133, 1500, and 1850 Hz. With the load cell base and cantilever beam in the unblocked condition, the observed natural frequencies occurred at about 48, 1500, and 1850 Hz. The 133- or 48-Hz and the 1500-Hz natural frequencies were easily observed in the load cell output signal. However, the 1850-Hz natural frequency could only be observed after application of the first step in the dynamic compensation procedure. A lumped parameter, three-degree-of-freedom model, which adequately represents the structure of Fig. 1, is shown in Fig. 3.

For the sake of simplicity, the damping elements shown in Fig. 3 are assumed to be viscous energy dissipation mechanisms. The magnitude of a viscous damping force is proportional to and acts in phase with velocity. Actually, the damping force mechanisms of the structure shown in Fig. 1 were caused by structural deformations and these forces are not viscous. Structural deformation damping forces are proportional to the degree of deformation or strain and act in phase with velocity. However, it was experimentally determined that the damping forces were so small that assumption of viscous damping forces resulted in no discrepancies between the analyses and experimental results.

The equations of motion for the model of Fig. 1 can be readily written in matrix form

$$\begin{bmatrix} M_1 & 0 & 0 \\ 0 & M_2 & 0 \\ 0 & 0 & M_3 \end{bmatrix} \begin{Bmatrix} \ddot{X}_1 \\ \ddot{X}_2 \\ \ddot{X}_3 \end{Bmatrix} + \begin{bmatrix} B_1 + B_2 & -B_2 & 0 \\ -B_2 & B_2 + B_3 & -B_3 \\ 0 & -B_3 & B_3 \end{bmatrix} \begin{Bmatrix} \dot{X}_1 \\ \dot{X}_2 \\ \dot{X}_3 \end{Bmatrix} + \begin{bmatrix} K_1 + K_2 & -K_2 & 0 \\ -K_2 & K_2 + K_3 & -K_3 \\ 0 & -K_3 & K_3 \end{bmatrix} \begin{Bmatrix} X_1 \\ X_2 \\ X_3 \end{Bmatrix} = \begin{Bmatrix} 0 \\ 0 \\ F(t) \end{Bmatrix} \quad (1)$$

where $\dot{X}$ and $\ddot{X}$ are the first and second time derivatives of X, respectively. It should be noted that only the transient solutions to Eq. (1) are needed since this report is concerned with force data distortions caused by the

transient response of the force measurement system structure. The transient solutions to Eq. (1) are of the form (Ref. 4)

$$X_i = \sum_{r=1}^{3} C_{ir} \exp(-\alpha_r t) \sin(\omega_r t + \psi_{ir}), \; i = 1, 2, 3 \qquad (2)$$

where the subscript, ir, is to be interpreted as the response at coordinate i caused by the natural frequency r, C is the peak amplitude, α is the attenuation constant, ψ is the phase shift, and

ω_1 = 133 Hz - with load cell base blocked

ω_1 = 48 Hz - with load cell base unblocked

ω_2 = 1500 Hz

ω_2 = 1850 Hz

It is precisely the transient responses of Eq. (2) that distort the load cell signal, and it is these distortions that must be eliminated by the hybrid dynamic compensation technique.

3.2 DYNAMIC COMPENSATION

Two independent but complementary dynamic compensation techniques have been combined to yield the so-called hybrid technique (Refs. 1 through 3). The first independent technique is termed the reaction force summation technique or accelerometer compensation technique. This technique utilizes the summation of the load cell signal and an accelerometer signal, mounted in proximity to the active end of the load cell, to eliminate distortions caused by (1) base motions (transient or steady-state) of the load cell and (2) the first natural frequency attributable to the structure forward of the active end of the load cell. The second independent technique is termed the computer compensation technique. The special purpose analog computer used in this technique is programmed with the inverse transfer function of the structure for one degree of freedom. Several stages of computer compensation can be used to compensate for several natural frequencies attributable to the structure forward of the active end of the load cell.

3.2.1 Elimination of Load Cell Base Motion Distortion–Compensation for the First Mode Natural Frequency

It is instructive to add the second and third equations represented in matrix form in Eq. (1). This addition yields

$$M_2\ddot{X}_2 + M_3\ddot{X}_3 + B_2(\dot{X}_2 - \dot{X}_1) + K_2(X_2 - X_1) = F(t) \qquad (3)$$

From Eq. (3) it can be seen that if the structure could be instrumented to measure the reaction force terms on the left side of Eq. (3), then these terms could be added and would identically equal the input force, F(t). A most important point to note is that the determination of the input force by this summation is entirely independent of the absolute motions of the load cell base but is dependent only upon the relative motion of the active end of the load cell with respect to its base. It is this relative motion that will compress or extend the load cell to produce an output signal.

Now, examine the damping term in Eq. (3). This damping force is caused by deformations of the load cell structure and is always quite small. The damping force term, therefore, may be neglected, and this simplification is shown experimentally in Section V to introduce no measurable error. Equation (3) may, therefore, be simplified to:

$$M_2 \ddot{X}_2 + M_3 \ddot{X}_3 + K_2 (X_2 - X_1) = F(t) \tag{4}$$

Examination of Eq. (4) shows that summation of the reaction terms on the left side of the equation will permit direct determination of the input force regardless of the absolute motions of the load cell base. For a rocket thrust stand, this would mean that the load cell signal could be made insensitive to thrust butt motions by proper addition of accelerometer signals.

3.2.2 Compensation for the Second Mode Natural Frequency

For the structure shown in Fig. 1, the amplitude of the third mode natural frequency was almost negligible compared to the first and second modes. This fact suggests that the third mode load cell signal distortion could have been caused by cross coupling of an off-axis natural frequency response such as a vibration orthogonal to the force measurement axis. Another possibility is that mass M_3 shown in Fig. 3 was actually quite small compared to M_1 and M_2 and, therefore, contributed only a small amplitude, $C_{23} - C_{13}$, to the load cell signal. In either case, when considering the second mode distortion and the model shown in Fig. 3, it is reasonable to assume that M_2 and M_3 experience approximately the same acceleration $\ddot{X}_2$. It now seems reasonable to mount an accelerometer on M_2 and to sum the accelerometer signal with the load cell signal to simultaneously eliminate both the first and second mode natural frequency distortions. However, the third mode natural frequency still remains in the summed signal so that Eq. (4) may be written

$$(M_2 + M_3) \ddot{X}_2 + K_2 (X_2 - X_1) = F(t) + (\text{third mode distortion}) \tag{5}$$

The elimination of natural frequency distortions by addition of the accelerometer and load cell signals is termed the reaction force summation or accelerometer compensation technique.

Now that the first and second mode distortions have been eliminated, the transient response of the force measurement system is a simplification of Eq. (2) to

$$X_i = (\text{third mode distortion}) = C_{i_3} \exp(-\alpha_3 t) \sin(\omega_3 t + \psi_{i_3}),\ i = 1, 2, 3 \tag{6}$$

The load cell transient signal is therefore of the form

$$(X_2 - Y_1) = (C_{2_3} - C_{1_3}) \exp(-\alpha_3 t) \sin(\omega_3 t + \psi) \tag{7}$$

This third mode natural frequency distortion could conceivably be reduced by filtering the reaction force summation signal. This attenuation approach to reduce the third mode distortion, however, is inferior to the analog computer compensation approach as explained in the next section.

3.2.3 Compensation for the Third Mode Natural Frequency

A linear system that possesses a transient time domain response described by Eq. (7) can be related to the following transfer function:

$$G_1(S) = A\left(\frac{1}{S^2 + 2\zeta_3\omega_3 + \omega_3^2}\right) \tag{8}$$

where A is a constant, and ζ_3 is the damping ratio associated with the third mode natural frequency and S is the Laplace transform variable.

Now, if a transfer function, $G_2(S)$, which is the inverse of $G_1(S)$, can be synthesized to operate on $G_1(S)$ such that the resultant time domain response is compensated, then the third mode natural frequency distortion would be eliminated. The ideal compensator transfer function is given by

$$G_2(S) = B(S^2 + 2\zeta_3\omega_3 S + \omega_3^2) \tag{9}$$

where B is a constant. The realization of $G_2(S)$ as expressed in Eq. (9) requires the use of differentiator circuitry that can easily be driven into saturation by high frequency signals and noise. However, use of approximate differentiator circuitry permits a practical synthesis of $G_2(S)$ with the form:

$$G_2(S) = B\left[\frac{(S^2 + 2\zeta_3\omega_3 S + \omega_3^2)}{(S + 10\omega_3)^2}\right] \tag{10}$$

where B is a constant and $10\omega_3$ is dictated by signal-to-noise considerations.

The transfer function, $G_2(S)$, can be synthesized by use of the analog computer circuitry shown in Fig. 4. The transfer function of this circuitry can be shown to be

$$G_2(S) = \left[\frac{R^2C_1^2 + bR^2C_1C_2 + R^2C_2^2}{RC_2}\right]\left[\frac{S^2 + \frac{(bRC_1 + 2RC_2)S + 1}{(R^2C_1^2 + bR^2C_1C_2 + R^2C_2^2)}}{(S + \frac{1}{RC_2})^2}\right] \tag{11}$$

where R, C_1, C_2 and b are chosen to satisfy Eq. (10).

The transfer function $G_1(S)$, can now be compensated by $G_2(S)$

$$G_1(S)\,G_2(S) = \frac{AB}{(S + 10\omega_3)^2}$$

which completes the compensation procedure. It should be noted that the computer compensation procedure has effectively extended the flat response bandwidth of the force measurement system by a factor of ten compared to the bandwidth of the reaction force summation compensated system. As previously mentioned, the first and second mode natural frequencies could have been eliminated by the reaction force summation technique and the third mode distortion eliminated by a filter. However, the cutoff frequency of the filter would have to be set at about $0.5\omega_3$ to $0.8\omega_3$ to eliminate the third mode oscillations. It is obvious that the compensation procedure yields a flat bandwidth at least an order of magnitude greater than the filter procedure. Therefore, the computer compensation procedure is much superior to the filter attenuation procedure. The hybrid combination of the reaction force summation and computer compensation techniques produces a significantly increased bandwidth as compared to the conventional load cell force measurement system.

A fourth mode natural frequency could conceivably be compensated by another stage of computer circuitry. However, experience has shown that compensation for four natural modes is about a practical limit for the hybrid compensation technique.

Because of the differentiating nature of the computer circuitry, a filter was used to attenuate high frequency noise before introduction of the signal to the computer. The filter is a linear phase type which is necessary for distortionless dynamic measurements (Ref. 1). The cutoff frequency was set at 9 kHz to minimize attenuation of force information.

SECTION IV
PROCEDURE

4.1 DYNAMIC COMPENSATION PROCEDURES

The steel sphere shown in Fig. 1 was first dropped upon the force measurement system from a moderate height to ensure that the force rating of the load cell and the acceleration rating of the accelerometer would not be exceeded. The height of the solenoid supporting the sphere was increased until the desired peak force was obtained. The natural frequencies to be compensated were also identified. As previously stated, the system shown in Fig. 1 exhibited three appreciable amplitude natural frequencies, 133, 1500, and 1850 Hz, with the cantilever beam blocked and 48, 1500, and 1850 Hz with the cantilever beam unblocked.

A previous study (Ref. 2) has shown that structural transient responses can produce dynamic force measurement errors greater than 70 percent in a conventional load cell force measurement system. This same study has also shown that application of the hybrid compensation technique could reduce this error to 2 or 4 percent. Another study (Ref. 3) has shown that proper adjustment of the hybrid compensation circuitry could be effected by exciting the natural frequencies of the force measurement structure with periodic impact forces and manipulating the circuit adjustments until the natural frequency distortions could no longer be visually detected on the oscilloscope. Therefore, the hybrid system adjustments were made for the system of Fig. 1 while that system was periodically excited with hammer raps.

4.2 FORCE CALIBRATION

After the dynamic compensation adjustments were completed, a deadweight was placed on top of the accelerometer housing to determine the system scale factor (lb_f/volt output). Experimental data (Ref. 3) have shown that accurate and precise dynamic force measurements are possible if the force measurement system is first dynamically compensated and then statically calibrated. However, no particular effort was expended in static calibration of the system shown in Fig. 1 since the object of this study was not to obtain particularly accurate force measurements but to show that identical dynamic force measurements could be recorded for two significantly different dynamic conditions of the load cell base (blocked and unblocked) with identical input forces in each situation.

A differential transformer with microinch measurement capabilities was used to monitor the cantilever beam motions. The transformer was calibrated with a micrometer dial with 0.0001-in. divisions.

SECTION V
RESULTS AND DISCUSSION

After the dynamic compensation and static calibration procedures were completed, the sphere support solenoid was positioned, and the light beam oscilloscope trigger circuit was activated.

Repeatable forces were introduced to the measurement system by impact of the 2.31-lb steel sphere. The sphere was dropped from precisely the same height each time by the electromagnet solenoid. With the same force applied each time, the repeatability of the force measurement signal, as a function of load cell base motions, was investigated by first blocking and then unblocking the cantilever.

From previous experience it was known that the impact force characteristics (peak force and total force-time duration) would be greatly dependent upon the characteristics of the resilient material upon which the sphere impacted. It was suspected that progressive deterioration of the resilient material caused by successive impacts could result in nonrepeatable forces. The inability to produce repeatable forces would negate the entire experiment. To illustrate the dependency of the force characteristics upon the conditions of the impacted surface, the data of Fig. 5 were recorded. The force-time function shown in Fig. 5a resulted from sphere impact directly upon the rubber-cork material shown in Fig. 1. A piece of ordinary note paper was next placed upon the rubber-cork, and sphere impact subsequently produced the force-time function shown in Fig. 5b. The peak force recorded in Fig. 5b is 128 lb less than that recorded in Fig. 5a, which vividly illustrates the dependency of the force-time function upon the impact surface conditions. Three impacts upon the rubber-cork material were recorded to show the repeatability of the data of Fig. 5a. The three photographs were precisely the same. Three impacts upon a sheet of paper were also recorded, and the results were precisely the same as Fig. 5b. The sensitivity of the force measurement system, as illustrated by the data of Fig. 5, showed that the system should easily reveal sensitivity or insensitivity to load cell base motions. The force measurement system was then subjected to a series of impacts to illustrate the effects of different dynamic conditions at the load cell base. Repeatable forces could not be obtained after six impacts because of deterioration of the rubber-cork material.

With the cantilever blocked, sphere impact produced the force-time function shown in Fig. 6a. With the cantilever unblocked, sphere impact produced the force-time function shown in Fig. 6b. Expanded time scale photographs of Figs. 6a and b are shown in Figs. 6c and d, respectively. The force-time functions are seen to be precisely identical regardless of the motions of the load cell base (cantilever). The load cell base motion corresponding to the data of Figs. 6a and c is shown in Fig. 6e, and the motion corresponding to the data of Figs. 6b and d is shown in Fig. 6f. It can be seen that the load cell base motion recorded in Fig. 6e is an order of magnitude less than that recorded in Fig. 6f, but the recorded force-time function is identical for the blocked and unblocked load cell base. The conventional load cell signal for the blocked load cell base is shown in Fig. 6g, and the load cell signal for the unblocked condition is shown in Fig. 6h. The distortion caused by load cell base motion is shown to be larger in Fig. 6h than in Fig. 6g since the load cell base motion is much greater. The natural frequency corresponding to the impacted mass and load cell spring constant (1500 Hz) about equally distorts the load cell data of Figs. 6g and h. The 1850-Hz distortion is not discernible in the data of Figs. 6g and h but could be observed in the output signal of the load cell and accelerometer summed signals. The computer compensation circuitry was used to eliminate the 1850-Hz distortion. It should also be noted that the peak force indicated in Fig. 6g is 3304 lb, whereas the peak force indicated in Fig. 6h is 2297 lb, a discrepancy of 1007 lb. The actual peak force, 2472 lb, is given by the data recorded in Figs. 6c and d. The data shown in Fig. 7 represent the hybrid system force measurement signal for a peak impact force of 4654 lb. The cantilever was unblocked, and maximum load cell base motion was about 0.25 in. peak to peak. The force measurement signal can be seen to be undistorted even under the influence of this severe dynamic force.

Perusal of Figs. 6a through h shows conclusively that utilization of hybrid dynamic compensation techniques with the force measurement structure of Fig. 1 has permitted repeatable dynamic force measurements to be made regardless of load cell base motions and the transient structural responses.

In Section 3.2.1 the assumption was made that the damping coefficient, B_2, was negligibly small. If B_2 had not been negligibly small, then the compensated force measurement data of Figs. 5a, 5b, 6c, 6d, and 7 would have exhibited a residual 1500-Hz distortion since the summation of the load cell and accelerometer signals does not account for damping forces (Ref. 2). However, the compensated data show that there is no residual 1500-Hz distortion so that the assumption that B_2 was viscous or even negligible was justified.

SECTION VI
SUMMARY OF RESULTS AND CONCLUSIONS

A conventional load cell force measurement system was subjected to quite severe impact-type dynamic forces. Peak force levels up to 4654 lb with fast rise times to 300 μsec and total force duration times as short as 900 μsec were imparted to the system by an impacting steel sphere weighing 2.31 lb. These impact forces excited the structural natural frequencies of the force measurement system. Therefore, the load cell signal was badly distorted so that it was impossible to measure the actual dynamic force.

Significantly different dynamic conditions were imposed on the load cell base by blocking or unblocking the base. Load cell base motions were restricted by the blocked condition, whereas large amplitude base motions were possible in the unblocked condition. With identical impact forces imparted to the system in first the blocked and then the unblocked conditions, large peak load cell force measurement discrepancies were noted. The difference between the blocked measurement (3304 lb) and unblocked measurement (2297 lb) of peak force was as great as 1007 lb. This shows that in some cases conventional rocket thrust stand measurements could yield significant errors when dynamic force measurements are attempted.

This report has shown that repeatable dynamic force measurements are possible regardless of the blocked or unblocked condition of the load cell base when hybrid dynamic compensation techniques are utilized. With identical impact forces imparted to the force measurement system, there was no measurable discrepancy in the dynamic force measurement data in the blocked and unblocked conditions when hybrid techniques were used. This shows that use of hybrid compensation techniques could significantly upgrade the dynamic force measurement capabilities of certain rocket thrust stands or other force measurement systems.

Application of the hybrid technique is straightforward, and the dynamic compensation adjustments for this study required only about two minutes to complete.

REFERENCES

1. Crosswy, F. L. and Kalb, H. T. "Investigation of Dynamic Rocket Thrust Measurement Techniques." AEDC-TR-67-202 (AD823181), November 1967.

2. Crosswy, F. L. and Kalb, H. T. "Evaluation of a Static and Dynamic Rocket Thrust Measurement Technique." AEDC-TR-68-117, September 1968.

3. Crosswy, F. L. and Kalb, H. T. "Evaluation of an Impact Type Dynamic Force Calibration Technique for a Static and Dynamic Thrust Measurement System." AEDC-TR-68-202, to be published.

4. Chen, Y. Vibrations: Theoretical Methods. Addison-Wesley, Reading, Massachusetts, 1966.

APPENDIX
ILLUSTRATIONS

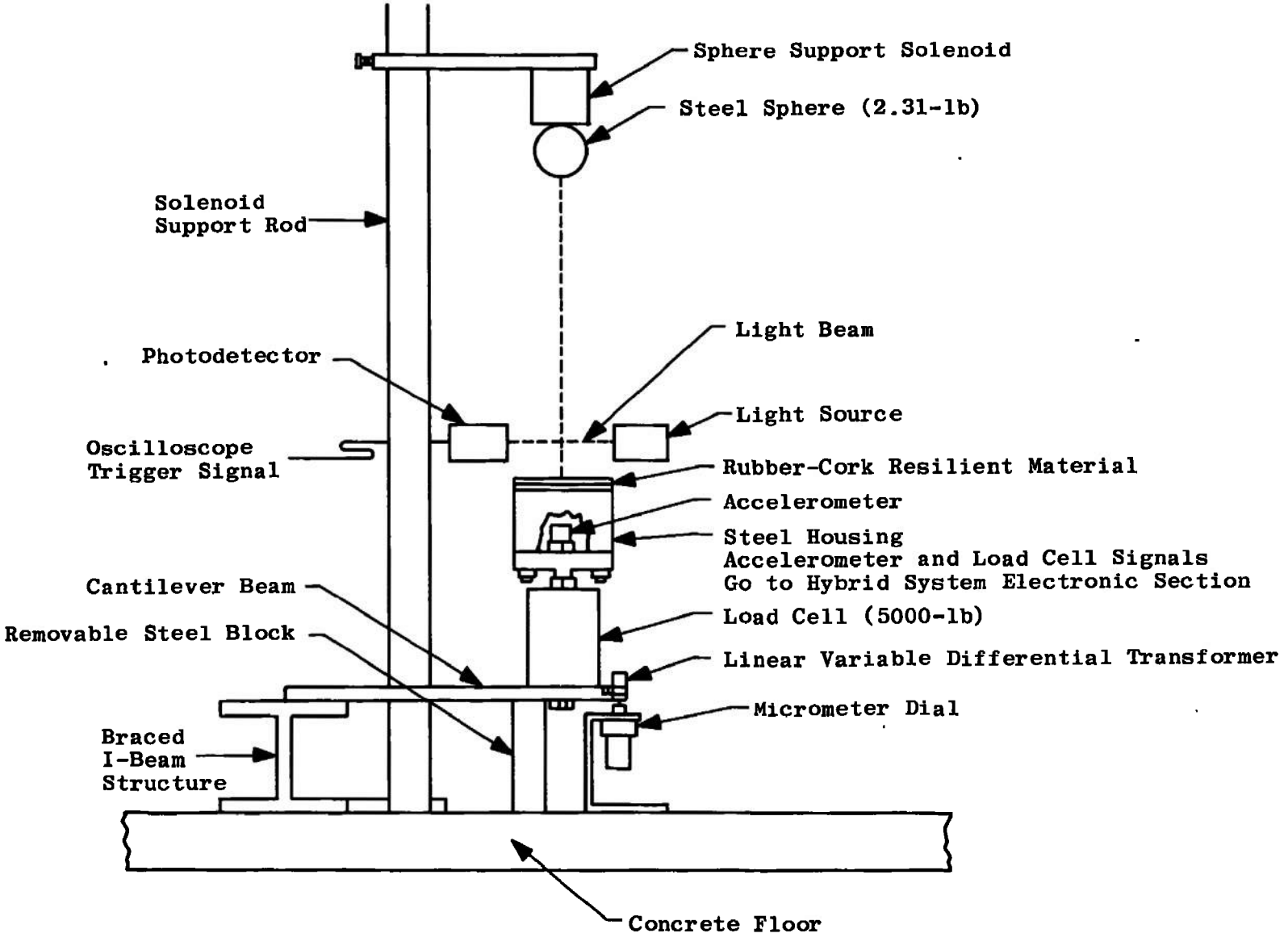

Fig. 1 Impact Force-Load Cell Base Motion Experiment

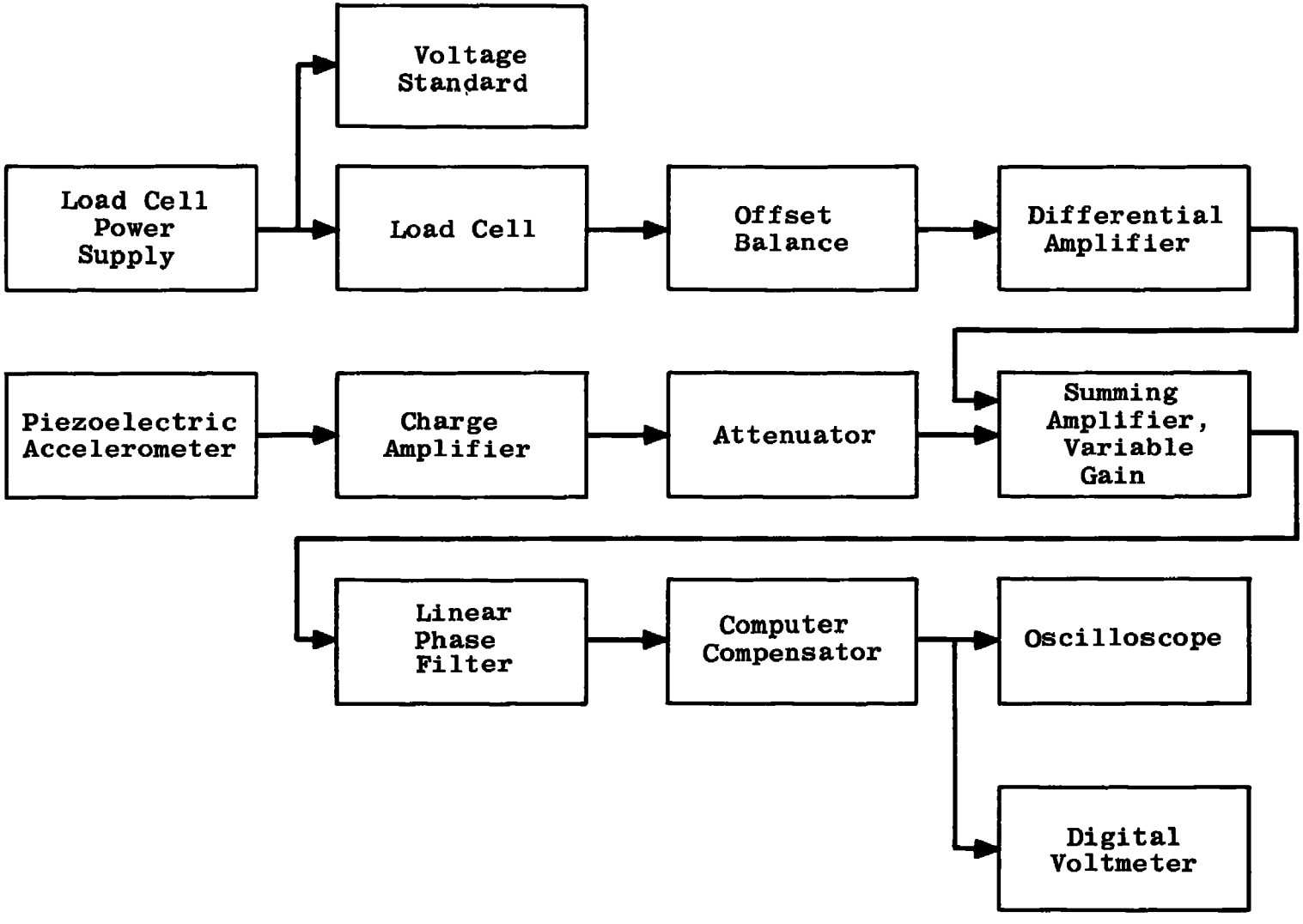

Fig. 2 Block Diagram of Hybrid System Transducers and Electronic Components

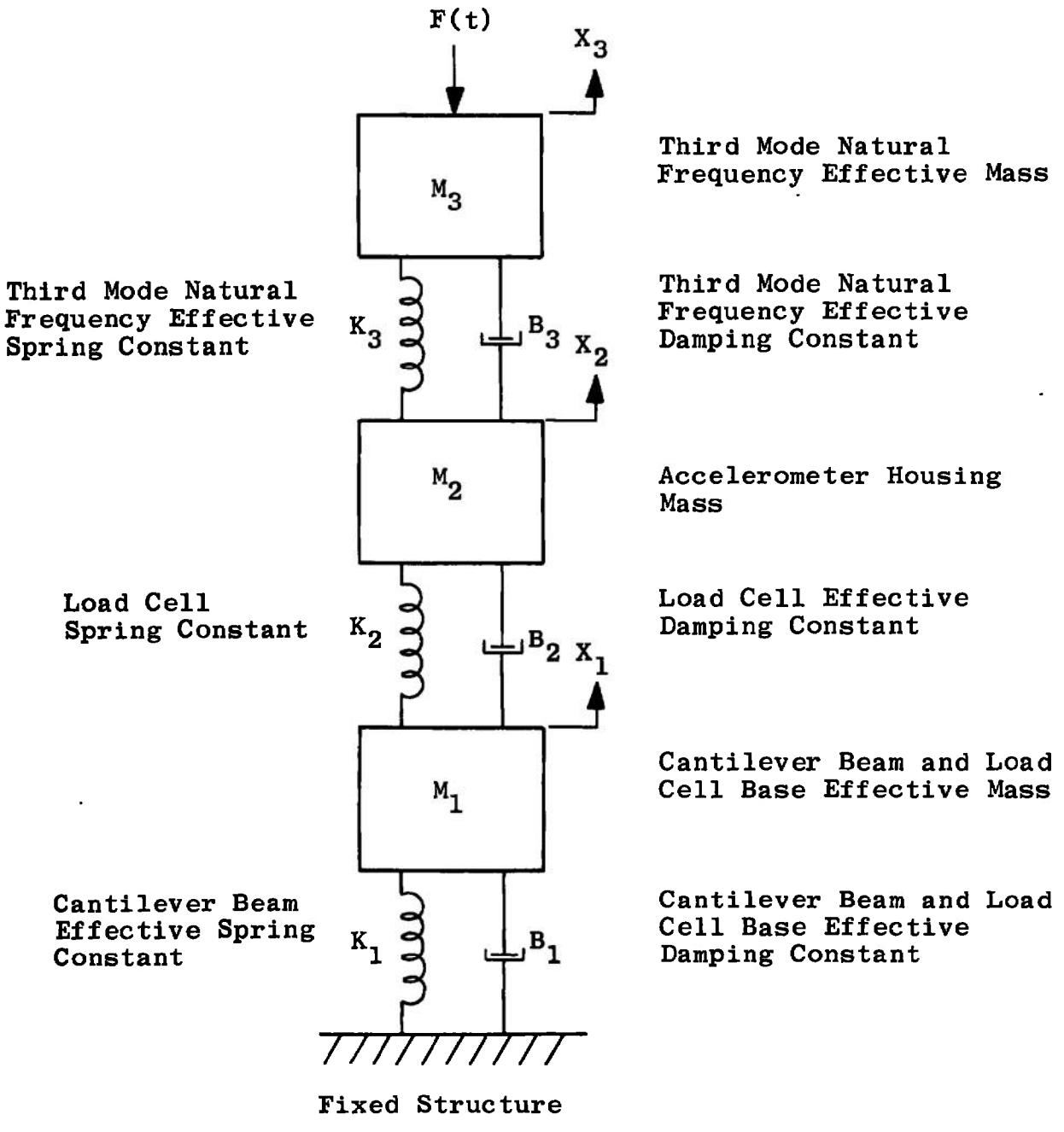

Fig. 3 Lumped Parameter Model of the Force Measurement System Structure

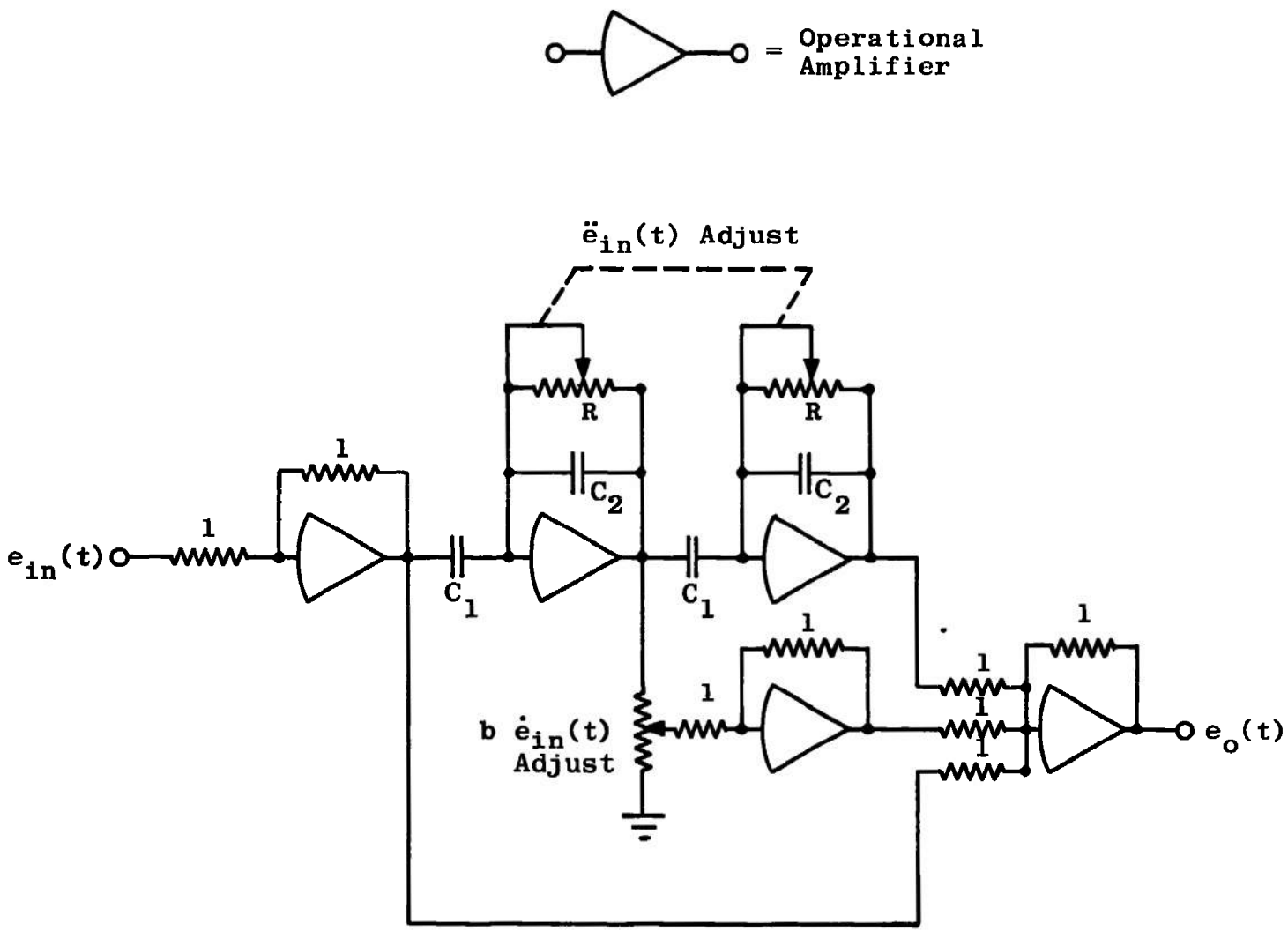

Fig. 4 Approximate Differentiator Circuitry

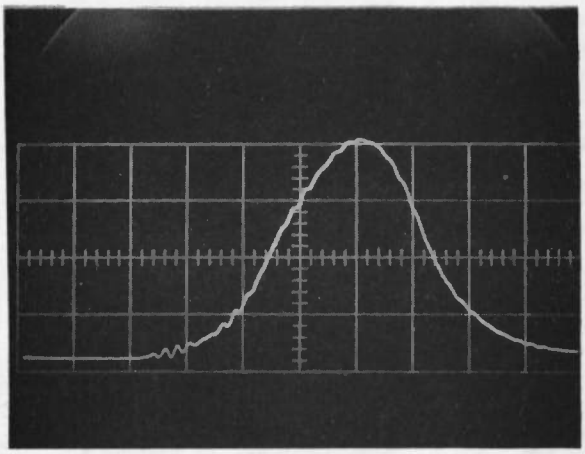

Horizontal Scale: 200 μsec/cm
Vertical Scale: 727 lb/cm
Peak Force: 2836 lb

a. Sphere Impact on Rubber-cork Material

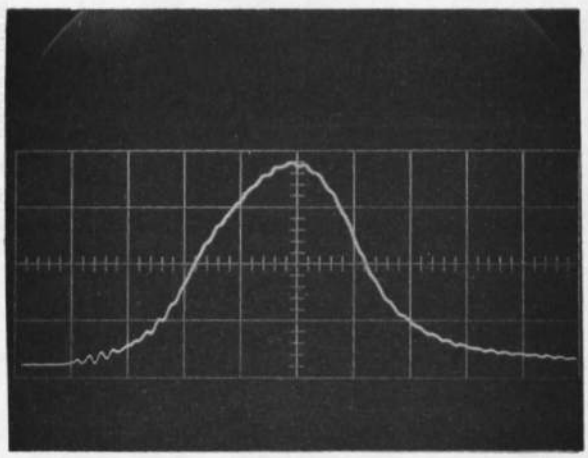

Horizontal Scale: 200 μsec/cm
Vertical Scale: 727 lb/cm
Peak Force: 2618 lb

b. Sphere Impact on Paper Backed by Rubber-cork

Fig. 5 Force-time Function Dependency upon Impact Surface Conditions

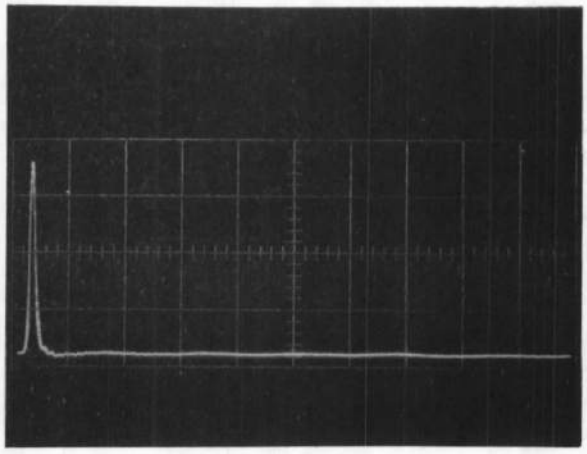

Horizontal Scale: 5 msec/cm
Vertical Scale: 727 lb/cm
Peak Force: 2472 lb

a. Hybrid System System Force Measurement Signal–Blocked Load Cell Base

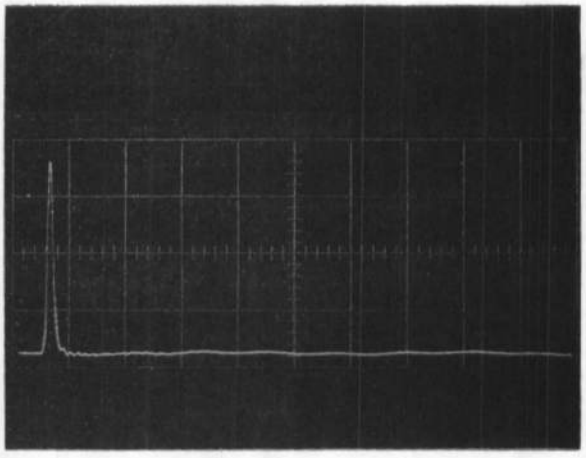

Horizontal Scale: 5 msec/cm
Vertical Scale: 727 lb/cm
Peak Force: 2472 lb

b. Hybrid System Force Measurement Signal–Unblocked Load Cell Base

Fig. 6 Measurement of the Impact Force of a 2.31 lb Sphere–Blocked and Unblocked Load Cell Base Conditions

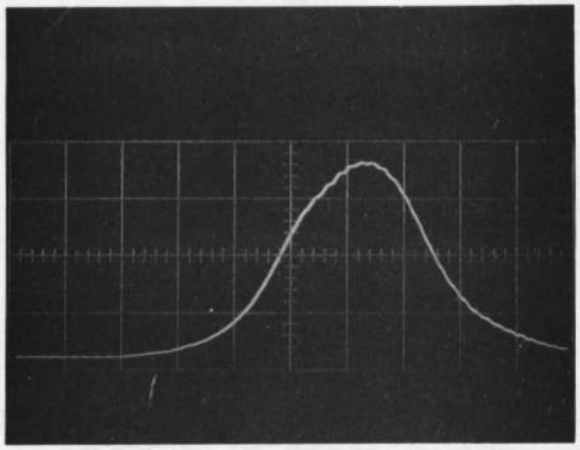

Horizontal Scale: 200 μsec/cm
Vertical Scale: 727 lb/cm
Peak Force: 2472 lb

c. Expanded Time Scale Photograph of Fig. 6a

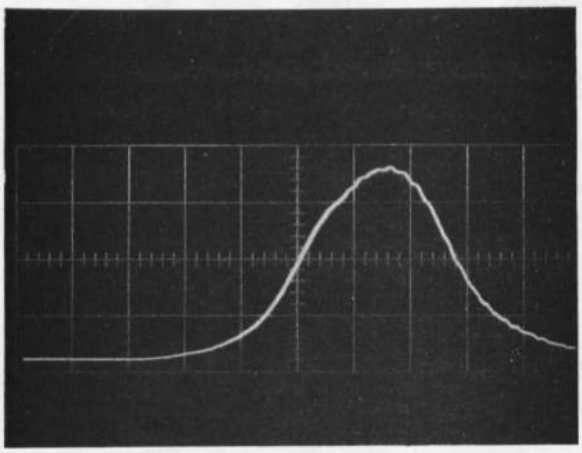

Horizontal Scale: 200 μsec/cm
Vertical Scale: 727 lb/cm
Peak Force: 2472 lb

d. Expanded Time Scale Photograph of Fig. 6b

Fig. 6 Continued

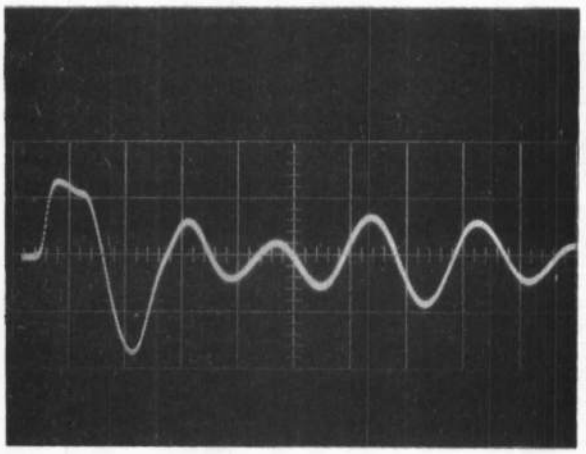

Horizontal Scale: 5 msec/cm
Vertical Scale: 0.0048 in./cm
Maximum Peak-to-Peak
Load Cell Base Displacement:
0.0144 in.

e. Blocked Load Cell Base Motion

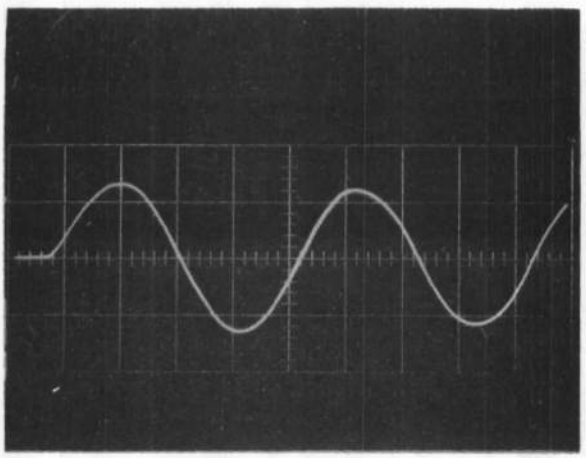

Horizontal Scale: 5 msec/cm
Vertical Scale: 0.048 in./cm
Maximum Peak-to-Peak
Load Cell Base Displacement:
0.125 in.

f. Unblocked Load Cell Base Motion

Fig. 6 Continued

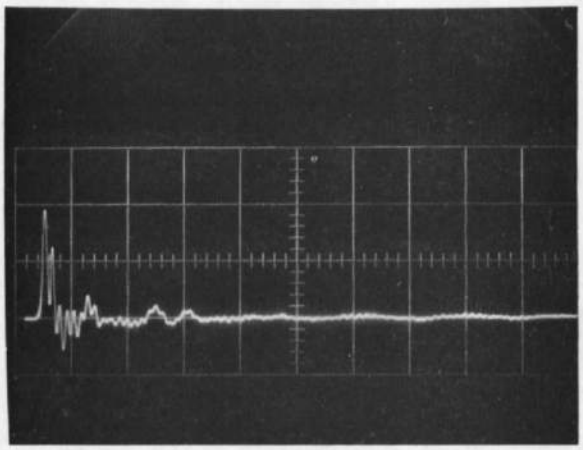

Horizontal Scale: 5 msec/cm
Vertical Scale: 1739 lb/cm
Peak Indicated Force: 3304 lb

g. Load Cell Signal–Blocked Load Cell Base

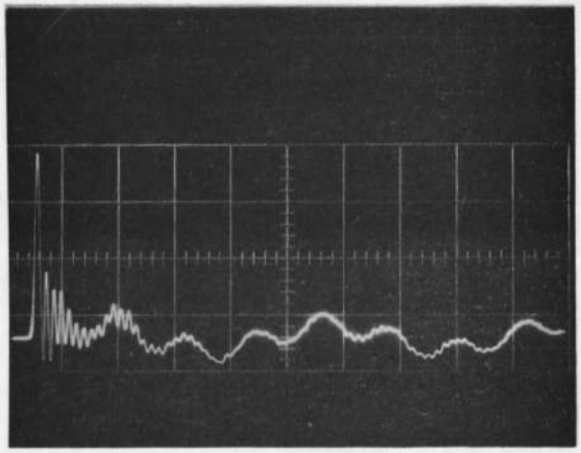

Horizontal Scale: 5 msec/cm
Vertical Scale: 696 lb/cm
Peak Indicated Force: 2297 lb

h. Load Cell Signal–Unblocked Load Cell Base

Fig. 6 Concluded

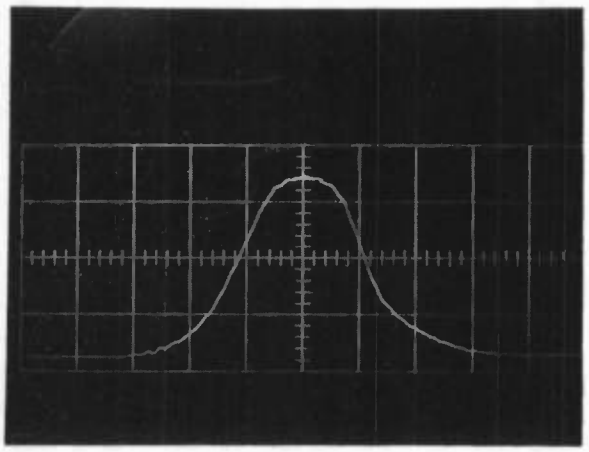

Horizontal Scale: 200 μsec/cm
Vertical Scale: 1455 lb/cm
Peak Force: 4654 lb
Maximum Peak-to-Peak
Load Cell Base
Displacement: Approximately
0.25 in.

Fig. 7 Hybrid System Force Measurement Signal with Unblocked Load Cell Base and 4654 lb Peak Impact Force

UNCLASSIFIED
Security Classification

DOCUMENT CONTROL DATA - R & D

(Security classification of title, body of abstract and indexing annotation must be entered when the overall report is classified)

1. ORIGINATING ACTIVITY *(Corporate author)* Arnold Engineering Development Center ARO, Inc., Operating Contractor Arnold Air Force Station, Tenn. 37389	2a. REPORT SECURITY CLASSIFICATION UNCLASSIFIED 2b. GROUP N/A

3. REPORT TITLE
PERFORMANCE OF A DYNAMICALLY COMPENSATED LOAD CELL FORCE MEASUREMENT SYSTEM

4. DESCRIPTIVE NOTES *(Type of report and inclusive dates)*
Final Report August to October 1967

5. AUTHOR(S) *(First name, middle initial, last name)*
F. L. Crosswy and H. T. Kalb, ARO, Inc.

6. REPORT DATE November 1968	7a. TOTAL NO. OF PAGES 31	7b. NO. OF REFS 4
8a. CONTRACT OR GRANT NO. F40600-69-C-0001 b. PROJECT NO. 5730 c. Program Element 62302F d. Task 04	9a. ORIGINATOR'S REPORT NUMBER(S) AEDC-TR-68-211 9b. OTHER REPORT NO(S) *(Any other numbers that may be assigned this report)* N/A	

10. DISTRIBUTION STATEMENT This document has been approved for public release and sale; its distribution is unlimited.

11. SUPPLEMENTARY NOTES Available in DDC.	12. SPONSORING MILITARY ACTIVITY Arnold Engineering Development Center, Air Force Systems Command, Arnold AF Station, Tenn. 37389

13. ABSTRACT

This report presents a theoretical description and an experimental evaluation of a dynamically compensated load cell force measurement system. Electronic compensation techniques were used to eliminate load cell signal distortions caused by large amplitude load cell base (thrust butt) motions and other structural transient responses of the force measurement device. The force measurement device was subjected to severe impact forces up to 4600 lb peak force with force rise times of 300 μsec and total force durations of 900 μsec. Load cell base motions caused by these impact forces approached 0.25 in., and the load cell signal was badly distorted. However, application of the compensation techniques eliminated these distortions, and dynamic force measurements could then be made regardless of load cell base motion and the structural response of the rest of the force measurement device.

DD FORM 1 NOV 65 1473

UNCLASSIFIED
Security Classification

14. KEY WORDS	LINK A		LINK B		LINK C	
	ROLE	WT	ROLE	WT	ROLE	WT
1 thrust measurement						
test facilities						
2 force measurement						
dynamic compensation						
distortion						
3. Load cells.						
4 Force measurement system						
17-5.						